

A Theoretical Investigation on the Wurster's Crown Analogue of 18-Crown-6

Andrew L. Sargent*,[†] Brian J. Mosley,[†] and John W. Sibert*,[‡]

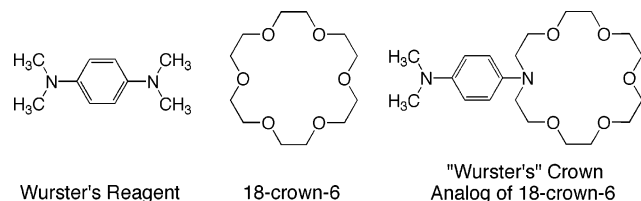
Department of Chemistry, East Carolina University, Greenville, North Carolina 27858, and
Department of Chemistry, University of Texas at Dallas, Richardson, Texas 75083

Received: September 30, 2005; In Final Form: December 14, 2005

An ab initio, quantum mechanical study of the Wurster's crown analogue of 18-crown-6 and its interactions with the alkali metal cations are presented. This study explores methods for accurately treating large, electron-rich species while providing an understanding of the molecular behavior of a representative member of this class of crowns. The molecular geometries, binding energies, and binding enthalpies are evaluated with methods similar to those reported for the analysis of 18-crown-6 and its alkali metal complexes to facilitate direct comparison. Hybrid density functional methods are applied to gauge the effects of electron correlation on the geometries of the electron-rich phenylenediamine moiety present in the Wurster's crowns. While the structure of the crown ether backbone is largely unperturbed by the incorporation of the redox active functionality, the alkali metal binding enthalpies are uniformly stronger for the Wurster's crown complexes, adding 1.8 to 5.1 kcal/mol to the strength of the interaction, depending on cation type. The additional strength, due to the exchange of an oxygen donor atom in the crown ether backbone by a nitrogen donor supplied by the redox group, is tightly coupled to the rotation of the dimethylaminophenyl group with respect to the plane of the macrocycle. Gas-phase selectivities favor the more highly charge-dense cations, while the explicit addition of only a few waters of hydration in the calculations recovers the selectivities expected in solution. The alkali metal binding affinity to the singly oxidized Wurster's crown is significantly diminished, while it is completely eliminated for the doubly oxidized ligand.

I. Introduction

The Wurster's azacrown ethers¹ are a class of redox-active macrocycles distinguished by the incorporation of the electron-rich *p*-phenylenediamine moiety within a macrocyclic framework.^{1–4} Structurally, they can be viewed as hybrids of the famed electroactive compound *N,N,N',N'*-tetramethyl-*p*-phenylenediamine, TMPD or Wurster's reagent,⁵ and classic crown ethers. Their design allows for an intimate association between a bound cation and the redox-active component of the macrocycle in the form of a chemical bond. As such, they are of interest in a variety of sensing, transport, and redox-switchable applications.



To achieve a fundamental understanding of the interaction between the redox-active component and cationic guest, we have undertaken a high-level ab initio theoretical analysis of a prototypical member of the Wurster's crowns, namely, the Wurster's crown analogue of 18-crown-6, and its alkali metal complexes. The major goals of this study are (1) to explore the mutual interactions between the electron-rich redox-active *p*-phenylenediamine unit and the bound guest; (2) to provide a

description at the molecular level for how the Wurster's crown functions as an electrochemical sensor; (3) to calculate the binding enthalpies for alkali metal complexes of Wurster's 18-crown-6 in the gas phase and compare them to those of 18-crown-6; and (4) to predict the alkali metal ion selectivity in solution.

While this study focuses specifically on the chemistry of a single macrocycle, its conclusions are of relevance not only to an emerging class of redox-active hosts, but to all ligating species that contain arylamine or aniline-like "N" donor atoms. For example, a large number of fluorescent sensors are based on the inclusion of an arylamine within a macrocycle.⁶ Further, and importantly, this study showcases a comparison of theoretical methods which should prove useful to those interested in modeling derivatized crown ethers and/or electron-rich species. It is worth noting that the first detailed ab initio theoretical study of alkali metal complexes of 18-crown-6 did not appear in the literature until 1994,⁷ testifying to the computational complexity of these systems. DFT studies on metal complexes of 18-crown-6 have also appeared;⁸ yet, until recently,⁹ there have been no reports on high-level theoretical studies of *derivatized* crowns, despite their predominance in the macrocyclic chemical literature.

II. Methods

As evidenced by the prior detailed ab initio theoretical studies of 18-crown-6 (18c6) and its metal complexes,^{7,8} simple crown ethers present a significant computational challenge. At the heart of this challenge are the number of atoms (43 in an alkali metal complex of 18c6) and the structural flexibility of the macrocyclic backbone. The Wurster's analogue of 18c6 (w18c6) increases the difficulty of the computational approach by expanding the

* sargenta@ecu.edu.

[†] East Carolina University.

[‡] University of Texas at Dallas.

total number of atoms in the system by 19 and decreasing the molecular symmetry from D_{3d} , in the best case, to nothing greater than C_s symmetry. Additionally, the electron-rich TMPD moiety requires a careful application of theory to yield structural parameters that are consistent with experiment. Small basis sets¹⁰ and uncorrelated wave functions¹¹ give rise to a combination of errors, including both over- and underpyramidalized nitrogen atoms, as well as twisting of the amino group relative to the plane of the benzene ring. Such geometric distortions are expected to have a significant impact on the Lewis basicity of the nitrogen donor atom. As outlined in detail below, two distinct procedures were therefore followed in this work to address the following separate objectives: (1) to produce results that could be compared to those from the study of 18c6, and (2) to report results that utilized a correlated wave function during the optimization steps to obtain better structural agreement with experiment and provide a more accurate description of the electron-rich nature of the Wurster's crowns.

To make a meaningful comparison of the properties and binding affinities of w18c6 to classical 18c6, the methods and basis sets employed must necessarily be commensurate. As such, the methods summarized in the following section are essentially the same as those reported by Glendening et al. for the study of 18c6,⁷ with discussion and detail highlighting any deviations from their original report.

Restricted Hartree–Fock (RHF) wave functions (or unrestricted Hartree–Fock, UHF, for the radical cations) were utilized to optimize molecular geometries in redundant internal coordinates¹² to the standard convergence thresholds, rather than the “tight” convergence thresholds used by Glendening et al. Motivating this change was the additional size of Wurster's crowns as well as new calculations, which reproduced the reported binding enthalpies for the alkali metal 18c6 complexes with the more relaxed convergence cutoffs. Frozen-core second-order Møller–Plesset perturbation theory (MP2) energies were evaluated at the RHF or UHF optimized geometries.

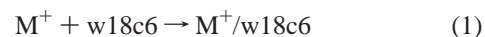
Following preliminary geometry optimizations with a standard 3-21G basis set, higher-level calculations were performed with a hybrid basis set, hereinafter designated “hyb_6-31+G*”, described by Glendening et al. This set used the standard 6-31+G* basis set for hydrogen, nitrogen, oxygen, lithium, and sodium, while for carbon, the standard 6-31G* basis set was used. For potassium, rubidium, and cesium, the ECP basis sets of Hay and Wadt¹³ were used where the (10s5p)/[3s2p] contractions of the valence space were augmented by six-term d-type polarization functions with exponents of $\alpha_d(\text{K}) = 0.48$, $\alpha_d(\text{Rb}) = 0.24$, and $\alpha_d(\text{Cs}) = 0.19$.

Extending the hyb_6-31+G* basis set used for 18c6 to the phenylenediamine moiety of the Wurster's crowns was handled in a straightforward manner wherein the nitrogen atoms maintained the full 6-31+G* representation while the carbons used the 6-31G* basis set. To determine the impact of this choice, the $\text{K}^+/\text{w18c6}$ complex was evaluated with a full 6-31+G* basis set on all atoms within the Wurster's crown and was found to produce a binding enthalpy that was within 1.0 kcal/mol of the hyb_6-31+G* result. Additionally, the difference in basis set had little influence on the structural features of the crown and its metal complex.

To investigate the influence of electron correlation on the molecular geometries and binding affinities of the Wurster's crowns and their associated alkali metal cation complexes, additional calculations were performed with density functional theory (DFT), where a wave function incorporating Becke's three-parameter hybrid functional (B3)¹⁴ was used along with

the Lee–Yang–Parr correlation functional (LYP).¹⁵ Preliminary geometry optimization calculations utilized a modest 6-31G basis set on all atoms except K, Rb, and Cs, where the ECP basis sets cited above were used without the polarization functions. Geometry optimization calculations using the hyb_6-31+G* basis set followed. This choice of wave function and basis set was influenced by studies of the vibrational spectrum of TMPD¹⁶ where the B3LYP/6-31G* level of theory was adequate to reproduce the C_{2h} molecular symmetry of the X-ray crystal structure.¹⁷ All calculations were performed within the *Gaussian 94*¹⁸ or *Gaussian 98*¹⁹ suite of programs.

The binding affinities of the Wurster's crowns for the alkali metal cations were evaluated by computing the energies of the gas-phase association reactions



where the free crown corresponds to the lowest-energy conformational isomer. Basis set superposition error was accounted for in an approximate manner by the full counterpoise correction of Boys and Bernardi.²⁰ In accord with the study of 18c6, scaled frequency calculations were evaluated at the RHF/3-21G level of theory (or the B3LYP/6-31G level, scaled to 0.98, for the DFT calculations) to obtain the vibrational contributions and enthalpy corrections at 298 K,²¹ and were also used to characterize the stationary points. With a single exception, namely, the radical cation of **8** at the B3LYP/6-31G level of theory, all structures reported herein correspond to genuine minima based on the absence of imaginary frequencies. Numerous attempts failed to locate the minima for **8** at the B3LYP/6-31G level. Evaluation of the B3LYP/hyb_6-31+G* frequencies of **8** revealed a genuine minimum. The thermal corrections to the enthalpy evaluated at these two levels of theory were within 0.07 kcal/mol of each other, and on these grounds, we justified use of the thermal correction evaluated at the lower level of theory. Naturally, the thermal corrections at the higher level were not evaluated on a routine basis as a matter of practicality to avoid overwhelming the available computational resources.

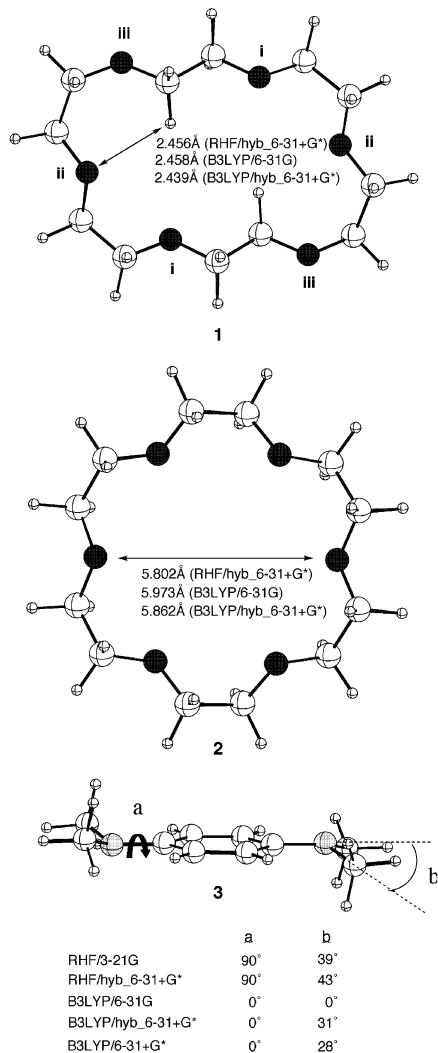
Atomic charges were calculated by the natural population analysis (NPA)/natural bond orbital (NBO) method.²² In these single-point calculations, pure five-term d-type polarization functions replaced the Cartesian six-term d-type functions of the hyb_6-31+G* basis set outlined above to decrease the total number of contracted basis functions in the calculations. Restrictions in the default implementations of the *Gaussian 94* and *Gaussian 98* NPA/NBO code limit the analysis to systems with fewer than 500 contracted basis functions—a limitation that can be accommodated through the use of the spherical-harmonic d-type polarization functions. Deformation densities were rendered through a modified version of the program MOPLOT.²³

III. Geometries and Binding Affinities

As a starting point for this study, we compare established methods for underivatized crowns to an alternative method to determine the minimum-energy structure of w18c6. The established methods allow for direct comparison of the structures and binding affinities reported herein to those reported by others.⁷ The alternative method utilizes a correlated wave function in an attempt to better model the electron-rich redox-active component in w18c6.

A. Uncomplexed w18c6. Previous studies⁷ of 18c6 singled out two isomers from among the many low-energy conformations sampled at room temperature: the C_i symmetry isomer,

1, which represents the global energy minimum in the gas and solid phases, and the D_{3d} isomer, 2, which is thought to be the conformation most frequently sampled in polar solvents and the one which possesses a nucleophilic cavity most suitable for

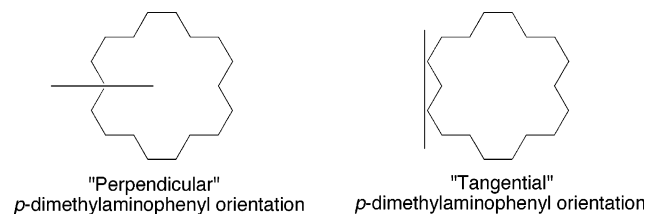


interactions with cationic guests.²⁴ Derivatization of 1 with Wurster's reagent, 3, reduces the symmetry from C_i to C_1 and produces three isomers by virtue of the three symmetry-unique heteroatoms, any one of which is, formally, a candidate for replacement by the phenylenediamine moiety. Two of the heteroatoms, i and ii, as labeled in structure 1, are endocyclic, with the latter participating in a weak transannular C—H...O interaction. The remaining symmetry-unique heteroatom, iii, is exocyclic. The optimized geometries of the corresponding w18c6 isomers are illustrated in structures 4, 5, and 6 of Figure 1, where the functionalization has occurred at heteroatoms i, ii, and iii, respectively.

Derivatization of 2 with Wurster's reagent reduces the D_{3d} symmetry of the parent macrocycle to C_s . In this symmetry, the dimethylaminophenyl substituent can adopt one of two possible orthogonal orientations with respect to the plane of the crown. Structures 7 and 8 of Figure 1 illustrate the respective optimized geometries.

The two distinct geometric orientations that result from the twisting of the redox group with respect to the perimeter of the macrocycle are important in the broad perspective of this work.

Clarification of the terminology used in reference to these orientations is given in the schematic below. The tangential



orientation retains much of the structure characteristic of TMPD. In the perpendicular orientation, the *p*-dimethylaminophenyl group is twisted by approximately 90° relative to the binding pocket of the macrocycle.

Table 1 reveals that the relative energetics of conformational isomers 4–8 are sensitive to the level of theory. Results from calculations on Wurster's reagent, 3, mirror this sensitivity. A geometry optimization of 3 with an RHF wave function results in a 90° rotation of one or both dimethylamino groups (depending on the quality of the basis set) relative to the plane of the phenyl ring and yields substantial sp^3 hybrid character at one or both nitrogen atoms. Similarly, geometry optimization of the Wurster's crown ether with an RHF wave function favors isomers 4–6 with a perpendicular *p*-dimethylaminophenyl orientation.

X-ray crystallographic data¹⁷ indicate that the dimethylamino groups in 3 are not perpendicular to the plane of the phenyl ring, as suggested by RHF calculations, but are more nearly coplanar with it. A modest degree of sp^3 hybrid character exists at the nitrogen atoms, yielding the overall S -shaped, C_{2h} symmetry shown in 3. Prior theoretical work^{16b} demonstrated that the B3LYP/6-31G* level of theory was sufficient to accurately reproduce the experimental geometry of TMPD. More extensive computational studies demonstrate that the molecular geometry is sensitive to the quality of the basis set as well as electron correlation effects. For example, optimization at the popular B3LYP/6-31G level of theory renders 3 completely flat, with D_{2h} symmetry. Consistent with this result, the two lowest-energy isomers of the Wurster's crown calculated at the B3LYP/6-31G level of theory (6 and 8) possess a planar arrangement of the α -methylene carbons of the crown with the dimethylaminophenyl group (note that Figure 1 illustrates the geometries optimized at the B3LYP/hyb_6-31+G* level and therefore does not show this planarity).

Only the combination of a correlated wave function and quality basis set such as hyb_6-31+G^* yields calculated structural parameters of Wurster's reagent that are consistent with the experimental data. Not surprisingly, application of the same level of theory to the Wurster's crown ether yields isomer

TABLE 1: Relative Energies (in kcal/mol) of Five Low-Energy Conformational Isomers of w18c6 Optimized at Different Levels of Theory

method	structure type ^a				
	4	5	6	7	8
RHF/3-21G	+3.7	0	+0.4	+17.0	+5.9
RHF/hyb_6-31+G*	+0.5	+1.4	0	+4.7	+3.0
MP2/hyb_6-31+G* ^b	0	+0.9	+1.2	+4.8	+3.3
B3LYP/6-31G	+2.6	+3.0	0	+11.8	+1.2
B3LYP/hyb_6-31+G*	+1.4	+2.5	+0.7	+4.8	0
B3LYP/6-31+G*	+1.9	+2.9	+1.9	+4.3	0

^a General structural types are identified by referencing a specific geometry-optimized structure reported herein. ^b Energy evaluated at RHF/hyb_6-31+G* optimized geometries.

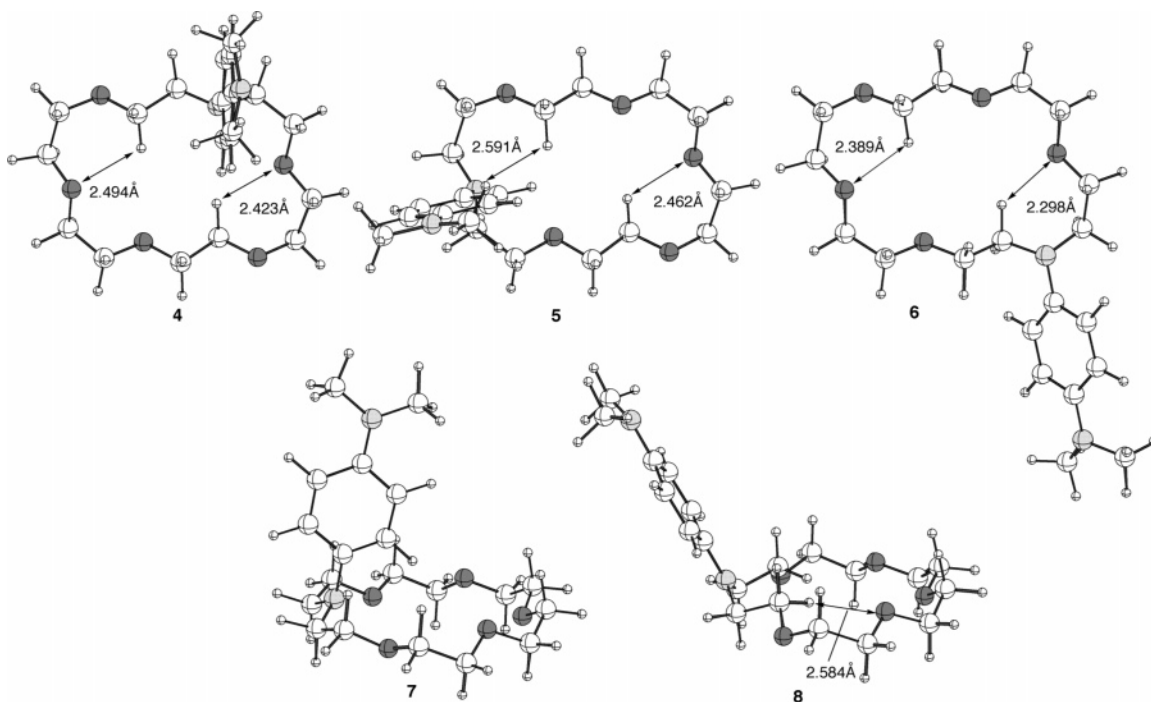


Figure 1. B3LYP/hyb_6-31+G* optimized geometries for various isomers of the Wurster's analogue of 18c6. Structures 4–6 were optimized without symmetry constraints, while 7 and 8 were optimized in C_s symmetry.

8, with the tangential orientation, as the global minimum. A lower level of theory fails to adequately accommodate the high electron repulsion inherent in the electron-rich redox group and therefore resorts to the 90° twist, to disrupt the π -orbital overlap, and/or excessive sp^3 hybridization, to dump electron density into lone pairs, in its structure.

That the local minima 4–6, evaluated at the B3LYP/hyb_6-31+G* level of theory, fail to adopt the tangential orientation is due, at least in part, to steric repulsion between hydrogens on the phenyl ring and those on the crown. The global minimum, **8**, diminishes this repulsion through a structural rearrangement that results in two exocyclic oxygen donor groups.

To summarize, we have explored two methods, RHF and DFT, to determine the minimum-energy structures of w18c6. Use of the RHF method was inspired by previous work on traditional crown ethers⁷ and deemed necessary in the present study to allow direct comparison of w18c6 to 18c6. As such, it was used extensively in subsequent sections to explore the alkali metal coordination of w18c6. However, the DFT methods with a flexible basis set provided a more accurate depiction of the molecular and electronic structure of the electron-rich phenylenediamine unit in w18c6 and were utilized to gauge the reliability of the RHF host–guest interactions.

B. w18c6 Complexes of Li^+ , Na^+ , K^+ , Rb^+ , and Cs^+ . The B3LYP/hyb_6-31+G* optimized molecular geometries of the w18c6 complexes of Li^+ , **9**, Na^+ , **10**, K^+ , **11**, Rb^+ , **12**, and Cs^+ , **13**, are shown in Figure 2. Remarkably, the coordination environment of each metal ion is nearly identical to that in the 18c6 complexes. The crown units in structures **9** and **10**, for instance, maintain the S_6 and C_1 symmetries, respectively, of the traditional crown ether complexes, while those in structures **11**, **12**, and **13** maintain the D_{3d} (**11**) and C_{3v} symmetries (**12**, **13**) of their crown ether/alkali metal counterparts. Functionalization of 18c6 with the Wurster's reagent therefore appears to have little impact on the structure of the host–guest interaction.

Of particular significance to the geometries of the w18c6 complexes is the perpendicular orientation of the *p*-dimethylaminophenyl group, which is rotated approximately 90° from

the orientation adopted by TMPD. Interestingly, results from geometry optimization calculations with RHF methods corroborate the perpendicular orientations of the DFT-optimized alkali metal ion complexes shown in Figure 2. The perpendicular orientation significantly enhances the Lewis basicity of the macrocyclic nitrogen atom because of the orthogonality of its lone pair with the π system of the dimethylaminophenyl group. In this orientation, the nitrogen donor atom behaves more like that in a traditional amine than that in aniline. In other words, the twist of the dimethylaminophenyl unit upon complexation disrupts the overlap of the macrocyclic N “p” orbital with the π system, thus enabling the N lone-pair density to be more effectively donated to the bound cation. The driving force for this twisting is the formation of a stronger N–metal bond. As a consequence of this study, we anticipate that the majority of Wurster's crown complexes^{1e} and, further, complexes of ligands that contain an aniline-like N atom, will generally show a similar geometric twist.²⁵ Left untwisted, the macrocyclic nitrogen's lone-pair density is delocalized throughout the phenyl π system, and the host–guest interaction is expected to be substantially diminished.²⁶ Of note, a comparable structural change presumably takes place in the metal chelation-driven twisting of fluorophores (i.e., twisted intramolecular charge transfer or TICT theory), a topic of considerable current interest.²⁷

To further explore the impact of the dimethylaminophenyl orientation on complex stability, we examined the K^+ complex in both the perpendicular, **11**, and tangential, **14**, orientations. The N–K distance in the calculated local minimum of the corresponding K^+ complex, **14**, is substantially elongated relative to that of the global minimum, **11**, (**11** K^+ –N = 3.012 Å, **14** K^+ –N = 3.689 Å, from Table 2), while the decreased binding affinities of **14** versus **11** (**11** = –69.4 kcal/mol, **14** = –58.8 kcal/mol, from Table 3) similarly reflect the diminished interaction.

The deformation density plots shown in Figure 3 support the claim that the Lewis basicity of the nitrogen donor atom decreases when the dimethylaminophenyl group twists 90° from the orientation shown in **11**. The four dashed contours shown

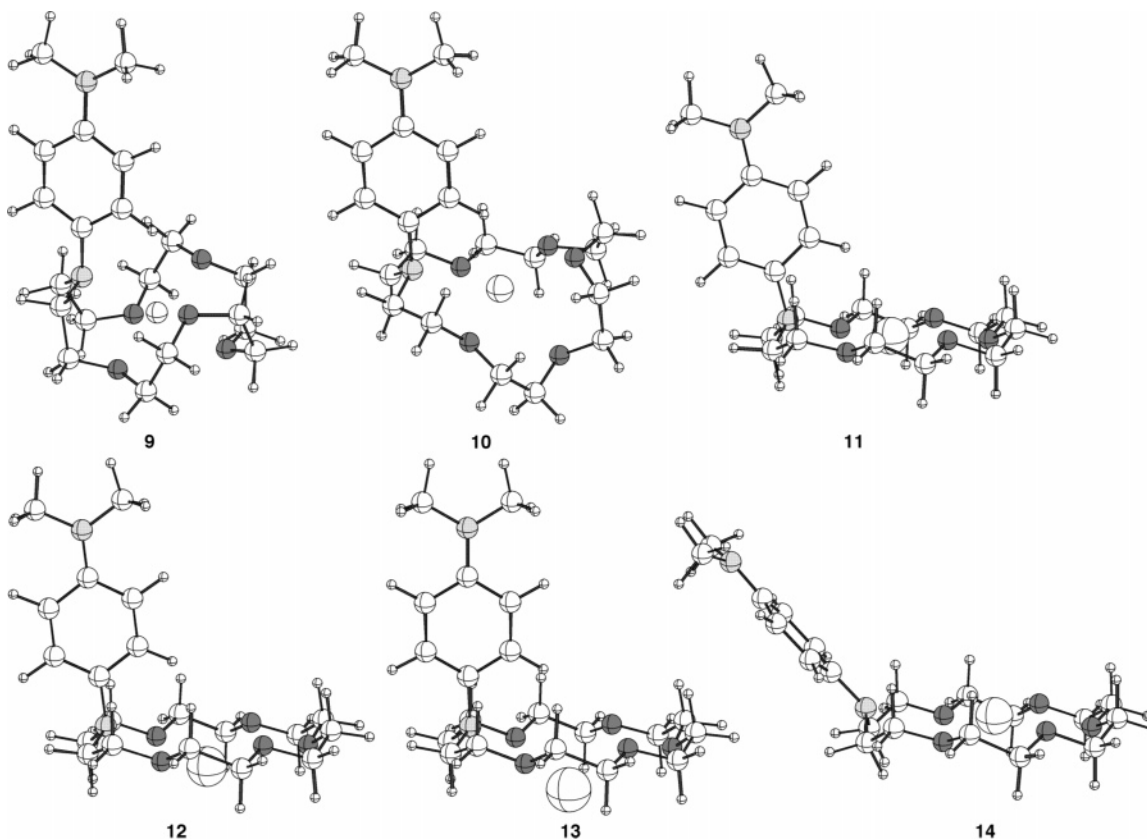


Figure 2. B3LYP/hyb_6-31+G* optimized geometries of the w18c6 complexes of Li⁺ (**9**), Na⁺ (**10**), K⁺ (**11** and **14**), Rb⁺ (**12**), and Cs⁺ (**13**). Structures **9**–**13** were optimized without symmetry constraints, while **14** utilized C_s symmetry to prevent rotation of the *p*-dimethylaminophenyl substituent.

in the nitrogen lone pair region of Figure 3a stands in contrast to the three contours shown in the corresponding region of Figure 3b and illustrates that more electron density is donated from the donor atom to the K⁺ atom in the former orientation than in the latter. The calculated natural atomic charges of the metal complex are also shown in Figure 3 and corroborate the conclusions drawn from the deformation density analysis. Less positive and more negative are the K⁺ and N-donor charges, respectively, in Figure 3a compared to the charges of the corresponding atoms in Figure 3b. That the N-donor atom has a more negative charge in Figure 3a corresponds to its greater electron density due to the lack of overlap of the lone-pair N orbital with the phenyl π system. The greater electron density of this donor atom therefore translates into a larger depletion in the lone-pair region in the difference density plot upon interaction with the metal ion compared to that for the conformational isomer shown in Figure 3b.

To ensure that this result is not a consequence of the fact that the hypothetical structure, which has the dimethylaminophenyl group twisted 90° from that shown in **11**, is not a minimum on any potential energy surface, deformation density calculations were performed with the structure shown in **14**, which is a true, albeit local, minima on the potential energy surface for the Wurster's K⁺ complex, and the corresponding plot is shown in Figure 3c. The hypothetical structure in these calculations involves a 90° rotation of the dimethylaminophenyl group in **14** and is illustrated in Figure 3d. The deformation densities and atomic charges are completely consistent with those shown in Figure 3a,b. Despite the nonequilibrium nature of the hypothetical structure in Figure 3d, the nitrogen is a better donor atom than that in the equilibrium structure of **14** shown

in Figure 3c. Again, the calculated natural atomic charges corroborate this view. We then conclude that the perpendicular orientation of the *p*-dimethylaminophenyl substituent serves to enhance complex stability by providing a better donor atom in the form of a localized lone pair on the macrocyclic N atom. Results obtained from deformation densities and atomic charges calculated at the RHF/hyb_6-31+G* level of theory were qualitatively consistent with those obtained at the B3LYP/hyb_6-31+G* level of theory shown in Figure 3.

C. Energetics of Metal Coordination: A Comparative Study. The total energies, binding energies, and binding enthalpies of free and complexed w18c6 are listed in Table 3. Interestingly, the alkali metal ion binding enthalpies of the Wurster's crowns are consistently stronger than those of the traditional crown ethers,⁷ adding 1.8–5.1 kcal/mol to the stability of the interaction, depending on the cation type. This result may not be obvious in light of the traditional view that aniline and its derivatives contain relatively poor N-donor functionalities. To probe this result further, K⁺ binding affinities were calculated for a series of azacrown ethers where, as shown in Table 4, a clear trend in the stabilities is revealed. In agreement with the experimental formation constants,²⁸ the calculated binding enthalpy for the K⁺ complex of aza-18-crown-6 is less stable than that for 18-crown-6 ($\Delta H = -66.6$ vs -67.6 kcal/mol). This result is understandable in light of the fact that a hard oxygen donor atom has been replaced by a relatively soft secondary amine. Consequently, the amine's interaction with the hard cation is significantly diminished. The binding affinity decreases further when the nitrogen heteroatom is derivatized with an electron-withdrawing phenyl group. The perpendicular orientation provides more stability to the complex

TABLE 2: Selected Bond Lengths (in Å) for w18c6 and Its Alkali Metal Complexes Using Uncorrelated and Correlated Electronic Structure Methods

RHF/hyb_6-31+G*						
structure type	M-N	C _{arene} -N _{proximal}	M-O (ave)	M-O (min)	M-O (max)	
w18c6	6	1.435				
w18c6 ⁺	6	1.336				
w18c6	8	1.398				
w18c6 ⁺	8	1.333				
Li ⁺ /w18c6	9	2.478	1.448	2.174	2.058	2.282
Li ⁺ /w18c6 ⁺	15	3.659	1.395	2.117	2.050	2.203
Na ⁺ /w18c6	10	2.678	1.444	2.479	2.386	2.664
Na ⁺ /w18c6 ⁺	16	3.207	1.427	2.387	2.356	2.421
K ⁺ /w18c6	11	3.022	1.444	2.820	2.793	2.843
K ⁺ /w18c6 ⁺	14	3.595	1.439	2.794	2.770	2.839
Rb ⁺ /w18c6	12	3.268	1.431	2.795	2.776	2.807
Rb ⁺ /w18c6 ⁺	18	3.172	1.443	2.983	2.951	3.006
Rb ⁺ /w18c6 ⁺	18	3.419	1.429	2.991	2.971	3.003
Cs ⁺ /w18c6	13	3.408	1.442	3.211	3.172	3.240
Cs ⁺ /w18c6 ⁺	19	3.676	1.427	3.238	3.201	3.256
B3LYP/6-31G						
structure type	M-N	C _{arene} -N _{proximal}	M-O (ave)	M-O (min)	M-O (max)	
w18c6	6	1.410				
w18c6 ⁺	6	1.373				
w18c6	8	1.411				
w18c6 ⁺	8^a	1.368				
Li ⁺ /w18c6	9	2.626	1.462	2.144	2.034	2.284
Li ⁺ /w18c6 ⁺	15	4.093	1.378	2.212	1.944	3.123
Na ⁺ /w18c6	10	2.639	1.464	2.441	2.349	2.599
Na ⁺ /w18c6 ⁺	16	4.337	1.377	2.321	2.271	2.371
K ⁺ /w18c6	11	3.070	1.463	2.823	2.789	2.859
K ⁺ /w18c6 ⁺	14	3.994	1.437	2.742	2.724	2.794
Rb ⁺ /w18c6	12	3.839	1.386	2.745	2.658	2.863
Rb ⁺ /w18c6 ⁺	12	3.124	1.462	2.899	2.866	2.930
Rb ⁺ /w18c6 ⁺	18	3.565	1.391	2.877	2.832	2.924
Cs ⁺ /w18c6	13	3.316	1.460	3.102	3.068	3.138
Cs ⁺ /w18c6 ⁺	19	3.910	1.388	3.132	3.057	3.234
B3LYP/hyb_6-31+G*						
structure type	M-N	C _{arene} -N _{proximal}	M-O (ave)	M-O (min)	M-O (max)	
w18c6	6	1.433				
w18c6 ⁺	6	1.363				
w18c6	8	1.404				
w18c6 ⁺	8	1.361				
Li ⁺ /w18c6	9	2.409	1.460	2.182	2.080	2.266
Li ⁺ /w18c6 ⁺	15	4.103	1.371	2.224	1.964	3.106
Na ⁺ /w18c6	10	2.629	1.457	2.485	2.396	2.620
Na ⁺ /w18c6 ⁺	16	3.948	1.375	2.354	2.304	2.404
K ⁺ /w18c6	11	3.012	1.456	2.832	2.801	2.859
K ⁺ /w18c6 ⁺	14	3.689	1.443	2.787	2.765	2.836
Rb ⁺ /w18c6	12	3.511	1.386	2.769	2.716	2.844
Rb ⁺ /w18c6 ⁺	12	3.146	1.455	2.971	2.936	2.995
Rb ⁺ /w18c6 ⁺	18	3.697	1.387	2.978	2.930	3.029
Cs ⁺ /w18c6	13	3.379	1.454	3.190	3.142	3.232
Cs ⁺ /w18c6 ⁺	19	4.050	1.384	3.232	3.151	3.317

^a Saddle point.

($\Delta H = -64.7$ kcal/mol) than the tangential orientation ($\Delta H = -55.8$ kcal/mol), but both are significantly below the value for aza-18c6.

Functionalization of the relatively soft secondary amine with electron-rich substituents can increase the hardness of this donor and enhance the interaction with a hard metal cation. Indeed, functionalization with *p*-amino- and *p*-dimethylaminophenyl groups results in sequentially stronger binding affinities ($\Delta H = -68.2$ and -69.4 kcal/mol) as expected on the basis of the increased electron-donating ability of these substituents. Func-

tionalization with an electron-withdrawing substituent, such as the *p*-nitrophenyl group, has the opposite effect: It enhances the softness of the macrocyclic nitrogen donor atom and diminishes the interaction with the hard metal cation. The calculated binding enthalpy, $\Delta H = -53.6$ kcal/mol, is less than that for the K⁺/aza-18-crown-6 complex ($\Delta H = -66.6$ kcal/mol). That the *p*-nitrophenyl group twists 30° from the perpendicular orientation is further evidence of the weakened Lewis basicity of the macrocyclic nitrogen donor atom.

While the tangential orientation of the *p*-dimethylaminophenyl-derivatized crown maintains a stronger K⁺ binding affinity than the phenyl derivative in the same orientation ($\Delta H = -58.8$ vs -55.8 kcal/mol), it is substantially weaker than the complex in the perpendicular orientation, emphasizing the binding interaction's geometric dependence on the donor group and the important role the perpendicular orientation plays in disrupting the electron delocalization of the donor atom's lone pair across the phenyl π system.

Importantly, the relative binding enthalpies listed in Table 4 demonstrate sensitivity to the level of theory. Comparison of data reveals that the RHF-based methods overestimate the binding affinities of the phenyl-derivatized crowns. We have seen that RHF methods provide a poor description of the geometric structure for the Wurster's crown and that this stems from its poor description of TMPD. A 90° rotation is observed around one or both dialkylamino groups (vide supra) in the Wurster's crown and Wurster's reagent alike. However, RHF methods provide a reasonable depiction of the molecular geometry for the alkali metal ion complexes with Wurster's crowns. The host/guest interaction is enhanced by the perpendicular orientation, and the RHF methods are better able to model this than they are the electron-rich, delocalized tangential orientation. As such, the MP2 energies calculated at the RHF optimized geometries of the phenyl-derivatized free crowns are too high and therefore result in binding energies (or enthalpies) that are too large. Consequently, the binding enthalpy for the K⁺ complex of phenyl-derivatized aza-18c6 is higher ($\Delta H = -73.3$ kcal/mol) than that for aza-18c6 ($\Delta H = -69.8$ kcal/mol), which goes against chemical intuition. The DFT methods, even with a modest 6-31G basis set, describes the electron-rich crown better (**6** is tangential at this level of theory, albeit excessively planar) and therefore gets the relative energetics of the series shown in Table 4 correct.

D. Oxidized w18c6 Structures and Binding Affinities. Wurster's reagent and, because of their structural relationship, the Wurster's crowns undergo two reversible one-electron oxidations that produce a delocalized radical cation²⁹ and a quinoid-like dication, respectively.³⁰ The first oxidation potentials of the Wurster's crown ethers and *p*-phenylenediamine-containing crown ethers have been shown to be sensitive to the presence of a bound cationic guest, shifting anodically upon binding.^{1e,3c,4b,31} Interestingly, electrochemical experiments indicate that, in general, the singly oxidized alkali metal ion complexes maintain their integrity despite the obvious Coulombic repulsions between the ligand radical cation and a cationic guest. All alkali metal complexes of w18c6 are reportedly unstable after the second oxidation of the ligand, as no change in the second oxidation potential of the complexes is ever observed with respect to that in the free w18c6. Similar electrochemical behavior was noted for the Ba²⁺ complex of a tetrathiafulvalene-derived crown.³² We investigated the alkali metal complexes of w18c6 in the singly and doubly oxidized states with computational tools to probe the effect of ligand oxidation state on complex stability and provide a description

TABLE 3: Total Energies, Binding Energies, and Binding Enthalpies of Free, Complexed, and Oxidized Wurster's Crowns^a

	structure type ^c	method	energy	ΔE^b	$\Delta H^{298,b}$
18c6	1	B3LYP/6-31G	-922.69662		
	1	B3LYP/hyb_6-31+G*	-923.01051		
	2	B3LYP/6-31G	-922.67984		
	2	B3LYP/hyb_6-31+G*	-923.00526		
Li ⁺ /18c6		B3LYP/hyb_6-31+G*	-930.44639	-91.0	-89.4
Na ⁺ /18c6		B3LYP/hyb_6-31+G*	-1085.22408	-79.1	-77.9
K ⁺ /18c6		B3LYP/hyb_6-31+G*	-951.09282	-68.5	-67.6
Rb ⁺ /18c6		B3LYP/hyb_6-31+G*	-946.80713	-55.3	-54.8
Cs ⁺ /18c6		B3LYP/hyb_6-31+G*	-942.81516	-44.3	-43.9
w18c6	4	RHF/3-21G	-1253.28830		
	4	RHF/hyb_6-31+G*	-1260.28382		
	4	MP2/hyb_6-31+G*	-1264.09834		
	4	B3LYP/6-31G	-1267.75653		
	4	B3LYP/hyb_6-31+G*	-1268.15419		
	5	RHF/3-21G	-1253.29424		
	5	RHF/hyb_6-31+G*	-1260.28238		
	5	MP2/hyb_6-31+G*	-1264.09689		
	5	B3LYP/6-31G	-1267.75597		
	5	B3LYP/hyb_6-31+G*	-1268.15244		
	6	RHF/3-21G	-1253.29355		
	6	RHF/hyb_6-31+G*	-1260.28454		
	6	MP2/hyb_6-31+G*	-1264.09642		
	6	B3LYP/6-31G	-1267.76074		
	6	B3LYP/hyb_6-31+G*	-1268.15531		
	7	RHF/3-21G	-1253.26718		
	7	RHF/hyb_6-31+G*	-1260.27711		
	7	MP2/hyb_6-31+G*	-1264.09074		
	7	B3LYP/6-31G	-1267.74187		
	7	B3LYP/hyb_6-31+G*	-1268.14878		
	8	RHF/3-21G	-1253.28476		
	8	RHF/hyb_6-31+G*	-1260.27969		
	8	MP2/hyb_6-31+G*	-1264.09314		
	8	B3LYP/6-31G	-1267.75877		
	8	B3LYP/hyb_6-31+G*	-1268.15646		
	6	UHF/3-21G	-1253.12234		
w18c6 ⁺	6	UHF/hyb_6-31+G*	-1260.10255		
	6	PMP2/hyb_6-31+G*	-1263.87238		
	6	UB3LYP/6-31G	-1267.56194		
	6	UB3LYP/hyb_6-31+G*	-1267.95002		
	8	UHF/3-21G	-1253.11604		
	8	UHF/hyb_6-31+G*	-1260.10622		
	8	PMP2/hyb_6-31+G*	-1263.89106		
	8	UB3LYP/6-31G	-1267.56290		
	8	UB3LYP/hyb_6-31+G*	-1267.95488		
	6	RHF/3-21G	-1252.78002		
w18c6 ⁺⁺	6	RHF/hyb_6-31+G*	-1259.78575		
	6	MP2/hyb_6-31+G*	-1263.58065		
	8	RHF/hyb_6-31+G*	-1259.76228		
	8	MP2/hyb_6-31+G*	-1263.54946		
	8	B3LYP/6-31G	-1267.21282		
	8	B3LYP/hyb_6-31+G*	-1267.59587		
Li ⁺ /w18c6	9	RHF/3-21G	-1260.71593		
	9	RHF/hyb_6-31+G*	-1267.67634		
	9	MP2/hyb_6-31+G*	-1271.52706	-106.9	-105.3
	9	B3LYP/6-31G	-1275.23374	-113.5	-112.0
	9	B3LYP/hyb_6-31+G*	-1275.60089	-96.1	-94.5
	10	RHF/3-21G	-1414.17247		
Na ⁺ /w18c6	10	RHF/hyb_6-31+G*	-1422.08027		
	10	MP2/hyb_6-31+G*	-1425.91809	-86.8	-85.6
	10	B3LYP/6-31G	-1430.00124	-93.4	-92.6
	10	B3LYP/hyb_6-31+G*	-1430.37622	-82.7	-81.8
K ⁺ /w18c6	11	RHF/3-21G	-1849.44314		
	11	RHF/hyb_6-31+G*	-1288.10295		
	11	MP2/hyb_6-31+G*	-1292.00362	-76.3	-75.5
	11	MP2/6-31+G*	-1292.04094	-75.3	-74.5
	11	B3LYP/6-31G	-1295.84722	-67.3	-66.7
	11	B3LYP/hyb_6-31+G*	-1296.24171	-70.1	-69.4
	11	B3LYP/6-31+G*	-1296.25716	-68.8	-68.2
	12	RHF/3-21G	-4177.98854		
Rb ⁺ /w18c6	12	RHF/hyb_6-31+G*	-1283.82085		
	12	MP2/hyb_6-31+G*	-1287.68299	-63.7	-63.2
	12	B3LYP/6-31G	-1291.56536	-56.8	-56.6
	12	B3LYP/hyb_6-31+G*	-1291.95628	-57.2	-56.9

TABLE 3: (Continued)

	structure type ^c	method	energy	ΔE^b	$\Delta H^{298,b}$
Cs ⁺ /w18c6	13	RHF/3-21G	-8783.33885		
	13	RHF/hyb_6-31+G*	-1279.83926		
	13	MP2/hyb_6-31+G*	-1283.70802	-54.6	-54.4
	13	B3LYP/6-31G	-1287.56984	-43.8	-43.9
	13	B3LYP/hyb_6-31+G*	-1287.96445	-46.3	-46.3
K ⁺ /w18c6	14	RHF/3-21G	-1849.41932		
	14	RHF/hyb_6-31+G*	-1288.08055		
	14	MP2/hyb_6-31+G*	-1291.98138	-62.8	-61.9
	14	B3LYP/6-31G	-1295.83325	-58.6	-57.7
	14	B3LYP/hyb_6-31+G*	-1296.22497	-59.7	-58.8
Li ⁺ /w18c6 ⁺	15	UHF/3-21G	-1260.44738		
	15	UHF/hyb_6-31+G*	-1267.40897		
	15	PMP2/hyb_6-31+G*	-1271.21016	-37.8	-37.1
	15	UB3LYP/6-31G	-1274.94557		
	15	UB3LYP/hyb_6-31+G*	-1275.30496	-37.8	-35.8
Na ⁺ /w18c6 ⁺	16	UHF/3-21G	-1413.90031		
	16	UHF/hyb_6-31+G*	-1421.80400		
	16	PMP2/hyb_6-31+G*	-1425.59258	-11.5	-12.1
	16	UB3LYP/6-31G	-1429.70490		
	16	UB3LYP/hyb_6-31+G*	-1430.07007	-17.4	-16.2
K ⁺ /w18c6 ⁺	17	UHF/3-21G	-1849.16574		
	17	UHF/hyb_6-31+G*	-1287.82623		
	17	PMP2/hyb_6-31+G*	-1291.67937	-2.0	-3.1
	17	UB3LYP/6-31G	-1295.54048		
	17	UB3LYP/hyb_6-31+G*	-1295.92565	1.4	2.5
Rb ⁺ /w18c6 ⁺	18	UHF/3-21G	-4177.71134		
	18	UHF/hyb_6-31+G*	-1283.54622		
	18	PMP2/hyb_6-31+G*	-1287.36119	8.9	7.6
	18	UB3LYP/6-31G	-1291.25668		
	18	UB3LYP/hyb_6-31+G*	-1291.64172	13.4	14.0
Cs ⁺ /w18c6 ⁺	19	UHF/3-21G	-8783.06510		
	19	UHF/hyb_6-31+G*	-1279.56726		
	19	PMP2/hyb_6-31+G*	-1283.38871	16.3	15.3
	19	UB3LYP/6-31G	-1287.26473		
	19	UB3LYP/hyb_6-31+G*	-1287.65357	21.8	22.3
Li ⁺ /w18c6 ⁺⁺		RHF/3-21G	-1260.01328		
		RHF/hyb_6-31+G*	-1266.97634		
		MP2/hyb_6-31+G*	-1270.77946	37.5	38.2
Na ⁺ /w18c6 ⁺⁺		RHF/3-21G	-1413.44424		
		RHF/hyb_6-31+G*	-1421.37938		
		MP2/hyb_6-31+G*	-1425.17626	52.3	52.3
K ⁺ /w18c6 ⁺⁺		RHF/3-21G	-1848.72318		
		RHF/hyb_6-31+G*	-1287.38541		
		MP2/hyb_6-31+G*	-1291.24701	73.8	73.6
Rb ⁺ /w18c6 ⁺⁺		RHF/3-21G	-4177.27052		
		RHF/hyb_6-31+G*	-1283.10361		
		MP2/hyb_6-31+G*	-1286.92948	83.6	83.5
Cs ⁺ /w18c6 ⁺⁺		RHF/3-21G	-8782.63516		
		RHF/hyb_6-31+G*	-1279.14298		
		MP2/hyb_6-31+G*	-1282.96470	81.8	81.9

^a Total energies are in au. Binding energies and enthalpies are in kcal mol⁻¹. Binding energies were evaluated relative to free metal cation and the lowest-energy free crown (in most cases, **6** for RHF/hyb_6-31+G* and B3LYP/6-31G; **8** for B3LYP/hyb_6-31+G*). RHF and DFT enthalpy corrections were determined using RHF/3-21G and B3LYP/6-31G harmonic vibrational frequencies, respectively. RHF energies for the 3-21G and hyb_6-31+G* basis sets as well as the DFT/B3LYP energies were evaluated at their optimal geometries. MP2/hyb_6-31+G* energies were calculated at the RHF/hyb_6-31+G* geometries. ^b Including the counterpoise correction for basis set superposition error for all entries. ^c General structural types are identified by referencing a specific geometry-optimized structure reported herein.

at the molecular level for how a Wurster's crown functions as an electrochemical sensor.

As noted above, oxidation of the Wurster's crown complexes results in the formation of a delocalized radical cation on the redox unit that repels the metal ion bound within the macrocyclic pocket. Consequently, each complex reorganizes its structure to put greater distance between these two localized positive charges. In the gas phase, the most charge-dense cation is expected to interact with the macroring donor atoms to the largest degree, and therefore, upon oxidation, we anticipate the largest increase in M⁺-N distance to occur for the Li⁺ complex. The calculated molecular geometries shown in Figure 4 support this view. The geometrical parameters listed in Table 2 show

that the M⁺-N distances increase by 1.69, 1.32, 0.50, 0.55, and 0.67 Å for the Li⁺, Na⁺, K⁺, Rb⁺, and Cs⁺ complexes, respectively. Note that the RHF methods significantly underestimate the M⁺-N distances, increasing them by only 1.18, 0.53, 0.25, 0.25, and 0.27 Å for the series. The calculated binding enthalpies, listed in Table 3, suggest that, while the complexes lose considerable stability upon oxidation, the energetics do not preclude weak association of the metal ion with the crown.³³

Because the singly oxidized ligand is a *delocalized* radical species,²⁹ there is potential for the lone pair to be maintained on the macroring N atom for donation to a cationic guest. If the lone pair is utilized in this manner, the metal ion complex

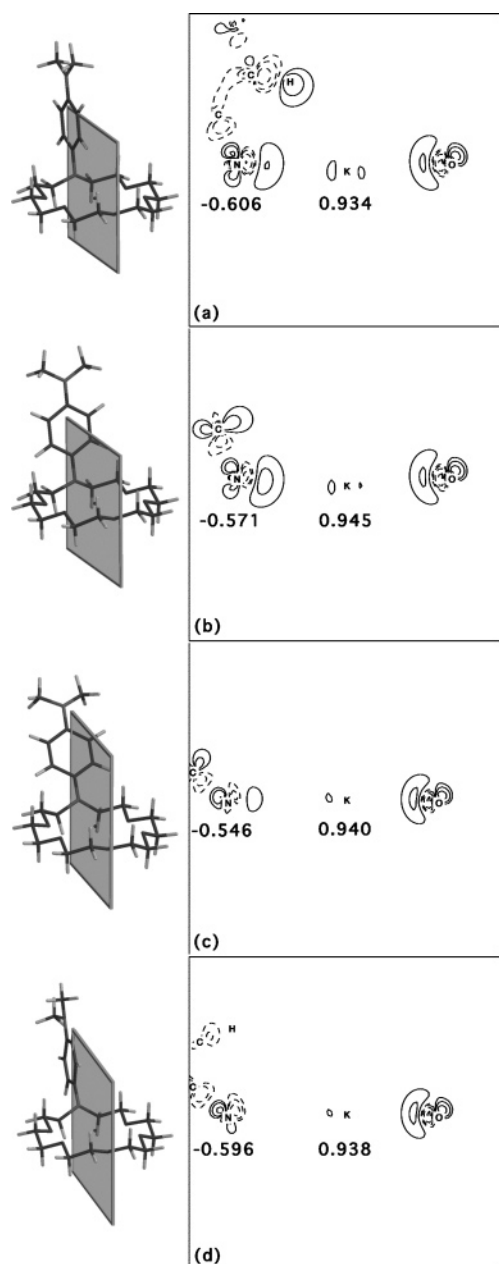
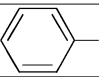
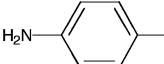
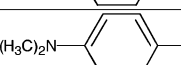
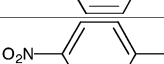
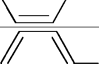
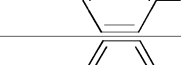


Figure 3. B3LYP/hyb_6-31+G* deformation density plots in the specified planes for (a) equilibrium structure **11**, (b) hypothetical structure derived from **11** by rotating the *p*-dimethylaminophenyl group by 90°, (c) equilibrium structure **14**, and (d) hypothetical structure derived from **14** by rotating the *p*-dimethylaminophenyl group by 90°. Promolecule densities for the neutral crown and cationic metal fragments were subtracted from the total density of the host–guest complex. The contours are geometric, with the value of the smallest positive and negative contours equal to $\pm 0.001953 e/a_0^3$. Negative contours are dashed. NPA atomic charges are shown for the nitrogen and potassium atoms.

would be expected to possess the perpendicular orientation for the reasons outlined in the preceding two sections. However, if the lone pair is instead used to stabilize the radical cation, the metal ion complex would be expected to adopt the tangential orientation where the orbital overlap with the π system of the phenylenediamine group is high. The RHF and DFT methods yield significantly different results in this respect. As shown in Figure 4, the DFT optimized geometries of **15–19** illustrate that the phenylenediamine moiety is not in the perpendicular orientation characteristic of the $M^+/w18c6$ complexes. In contrast, the RHF optimized geometries (not shown) all display

TABLE 4: Binding Enthalpies of Crown Ether–K⁺ Complexes^a

X	R	Orientation ^b	ΔH (kcal/mol) ^c		
			MP2-II	DFT-I	DFT-II
N	H–		-69.8	-65.4	-66.6
O			-71.5 ¹	-66.3	-67.6
N		Perpendicular	-73.3	-61.1	-64.7
N		Perpendicular	-74.5	-66.5	-68.2
N		Perpendicular	-75.5	-66.7	-69.4
N		Twisted 30° from Perpendicular	-67.0	-51.8	-53.6
N		Tangential	-60.4	-54.9	-55.8
N		Tangential	-61.9	-57.7	-58.8

^a Three levels of theory were employed: MP2/hyb_6-31+G* energies at RHF/hyb_6-31+G* optimized geometries; B3LYP/6-31G energies at B3LYP/6-31G optimized geometries; B3LYP/hyb_6-31+G* energies at B3LYP/hyb_6-31+G* optimized geometries. ^b See section IIIA for definitions of the perpendicular and tangential orientation. ^c Basis set definitions I and II correspond to 6-31G and hyb_6-31+G*, respectively.

the perpendicular orientation, with the exception of the lithium complex. Calculations on TMPD^+ reveal that although both RHF and DFT methods predict a flat, D_{2h} symmetry geometry for the radical cation, the energetic barrier associated with rotating one dimethylamine by 90° is nearly three times lower for the RHF methods than for the DFT methods. That the RHF methods fail to predict the correct geometry of neutral TMPD (*vide supra*) casts suspicion on its ability to predict the barrier to dimethylamino rotation in TMPD^+ and, by extension, the correct geometry in the metal ion complex with the Wurster's radical cation crown. On these grounds, we view the DFT results as more reliable and therefore conclude that the macrocyclic nitrogen lone pair provides greater stability to the molecule by preferentially stabilizing the radical cation. The partial twisting of the phenylenediamine moiety in **15–19** appears to be a consequence of steric repulsion between hydrogens on the phenyl ring and those on the crown.

Undoubtedly, the pronounced anodic shift in the first oxidation potential of the alkali metal complexes of *w18c6* versus that in the free ligand is due, in part, to intramolecular Coulombic repulsions between the cationic host and guest. However, an additional factor contributing to the observed anodic shift is the twisting of the dimethylaminophenyl substituent within the neutral crown upon complexation (with concomitant rehybridization of the macrocyclic N-donor atom). As stated previously, this twist serves to disrupt the overlap of the N “p” orbital with the aromatic π system, thereby leaving the macrocyclic N atom less able to stabilize the emergent

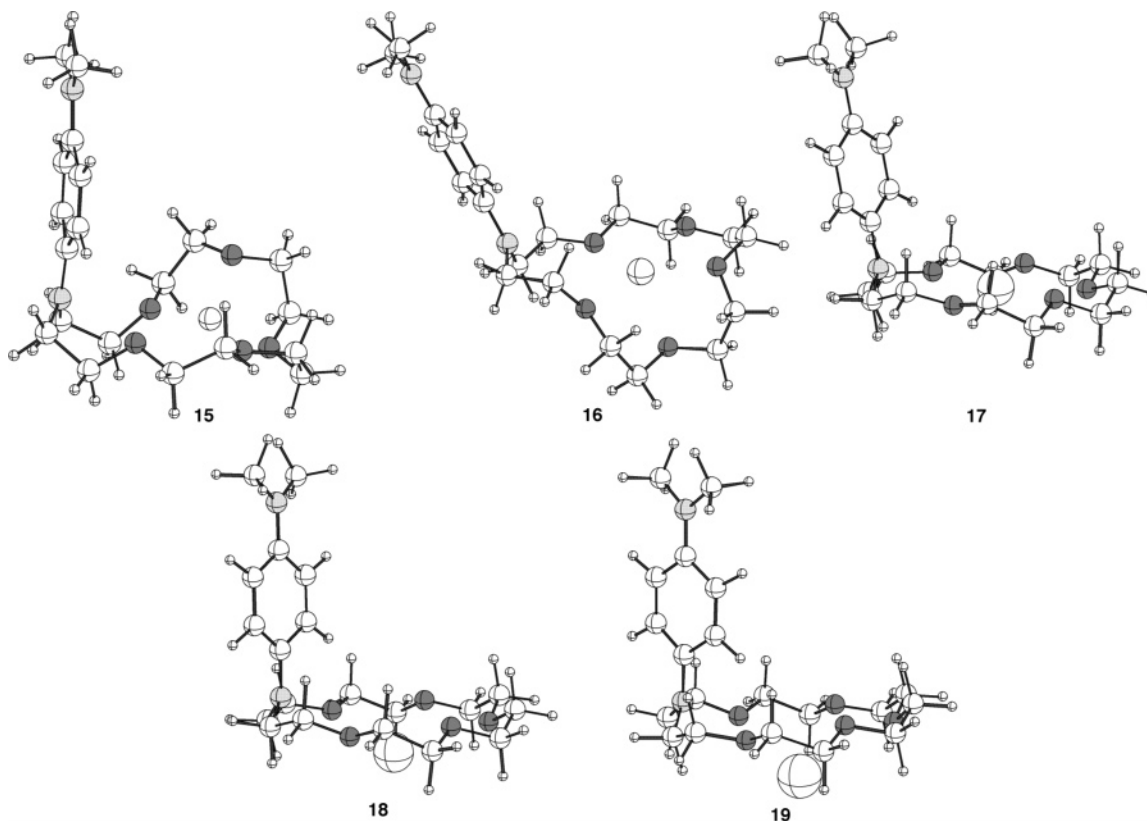


Figure 4. UB3LYP/hyb_6-31+G* optimized geometries of the oxidized Wurster's crown complexes of Li⁺ (**15**), Na⁺ (**16**), K⁺ (**17**), Rb⁺ (**18**), and Cs⁺ (**19**).

radical cation through π donation. It is the sum of these two factors that contributes to the observed shift in oxidation potential and accounts for how, at the molecular level, the crown senses the presence of a metal ion.

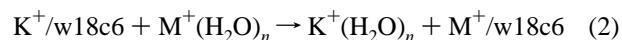
In contrast to the singly oxidized complexes, calculated binding enthalpies for the hypothetical doubly oxidized complexes show, in all cases, large positive values and, thus, complex instability. In addition to a greater charge (+1 vs +2), the dicationic redox center is now quinoid-like with the two positive charges localized on the N atoms. Thus, in this oxidation state, there is no incentive for interaction between the redox center and a bound cationic guest. This is consistent with experimental observation in that the second oxidation potentials of the Wurster's crowns generally remain unchanged in the presence of the alkali metal cations.^{1e}

IV. Cation Selectivity

As has been reported,^{1e,3c} the alkali metal cation that binds with the greatest strength in the crown pocket elicits the greatest shift in the first oxidation potential. Thus, w18c6, with a pocket size essentially equal to that in 18c6, is, like 18c6, selective for the potassium cation and, because of its ability to record the binding event electrochemically, can be viewed as a potassium ion sensor. However, the calculated binding enthalpies of w18c6 and 18c6 mirror the experimentally determined gas-phase selectivities, Na⁺ > K⁺ > Rb⁺ > Cs⁺ (Li⁺ was not included in the study).³⁴ In the gas phase, it is the charge density of the cation, rather than the ratio of ionic radius to the cavity size, that is the primary factor governing the affinity between host and guest. In solution, where the solvent and the crown compete for the metal ion, the overall selectivity is determined by a complex balance of factors that weighs the energy lost from

the desolvation of the free metal and crown fragments against that regained upon formation of the complex and its subsequent solvation.

In accord with the study of Glendening et al.,⁷ to investigate the role of solvent on the selectivity, we examined the reaction



where a metal cation M⁺, coordinated by $n = 0-4$ waters of hydration, exchanges with a K⁺ cation bound by a Wurster's crown. The exothermicity of the reaction is considered a relative measure of the selectivity of the metal cations. The more exothermic the reaction is for a given cluster size n , the more selective the Wurster's crown for the metal cation. Absent from eq 2 is the hydration of the complexes M⁺/w18c6. Glendening et al. determined that the hydration of the M⁺/18c6 complexes was expected to only weakly influence the energetics of the exchange reaction and consequently has little effect on the overall selectivities. We assume that the same will apply to the Wurster's analogues.

Figure 5a shows the reaction energies (ΔE) for eq 2 as a function of the cluster size n for w18c6. Results from the work of Glendening et al.⁷ on 18c6 are shown in Figure 5b for reference. The data for cluster size $n = 0$ mirror the gas-phase selectivities mentioned above. With increasing cluster size, the sequence changes to eventually yield the selectivities K⁺ > Na⁺ \approx Rb⁺ > Li⁺ \approx Cs⁺, which closely resemble the calculated selectivities for 18c6 shown in Figure 5b. Despite the qualitative similarities between the results presented in Figure 5a,b, an important fundamental difference is apparent. The ΔE values at $n = 4$ are less for w18c6 than for 18c6: For the former, ΔE (kcal/mol) = 9.8, 3.3, 4.0, and 11.0 for Li⁺, Na⁺, Rb⁺, and Cs⁺, respectively, while for the latter, they are 13.6, 4.9, 4.2,

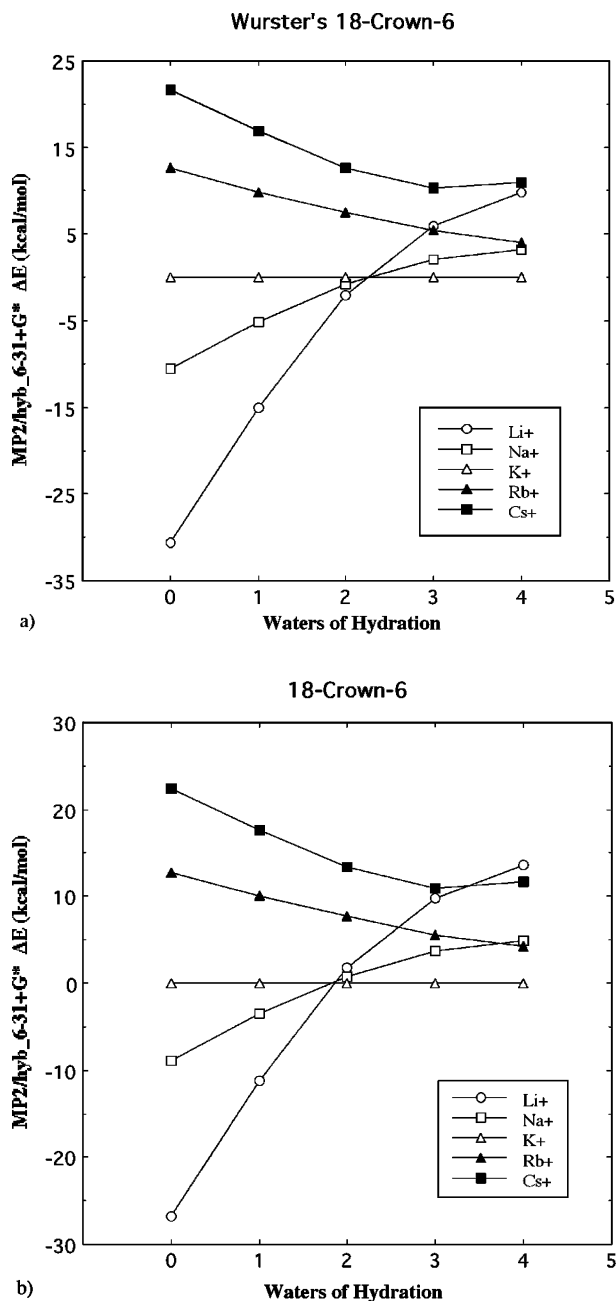


Figure 5. Reaction energies for the exchange reaction of eq 2 calculated at the MP2/hyb_6-31+G* level of theory at RHF/hyb_6-31+G* optimized geometries. (a) w18c6. (b) 18c6, where data points were replicated from data found in ref 7. Water cluster data were obtained from data found in ref 36.

and 11.7 for the same ions. This result suggests that, in solution, w18c6 is less selective for the potassium cation than 18c6. Further, the analysis is consistent with the generally greater binding enthalpies calculated for w18c6 versus 18c6 (see Table 3). The stronger donating ability of the macrocyclic N atom in w18c6 versus the ether functionality in 18c6 enhances the binding disproportionately in favor of better Lewis acids. This, therefore, has a greater effect on Li⁺ and Na⁺ complexes (the most charge dense and strongest Lewis acids in the alkali metal group) of w18c6, thereby decreasing the overall selectivity for K⁺. Indeed, for presumably a similar reason, early studies on nitrobenzyl-containing macrocyclic complexes revealed that the increased stability of alkali metal complexes upon reduction of the nitrobenzyl moiety was accompanied by a loss in selectivity.³⁵

V. Conclusion

We have used high-level ab initio methods to understand the coordination chemistry and electrochemical behavior of a Wurster's crown analogue of 18-crown-6. It was shown that replacement of a macrocyclic ether atom with an electron-rich arylamine moiety actually enhances metal complex stability. The enhanced stability is due, in part, to a 90° twist of the phenylenediamine substituent upon complexation where the twisted orientation serves to "free up" the lone pair on the macrocyclic N atom for donation to the captured metal ion. Deformation density plots of the alkali metal cation complexes support these conclusions. Interestingly, w18c6 was shown to be less selective for the potassium cation than 18c6 because of its stronger set of donor atoms preferentially stabilizing the more charge-dense alkali metal cations (e.g., Li⁺, Na⁺). Studies of complex stability with the ligand in the singly and doubly oxidized states provide an explanation for the observed voltammetric behavior exhibited by the alkali metal complexes of w18c6. The singly oxidized complexes remain intact, though weakened. In contrast, and consistent with a lack of shift in the second oxidation potential upon metal coordination, the doubly oxidized ligand does not form stable complexes with any of the alkali metal cations. The HF and post-HF methods used by Glendenning et al.⁷ for traditional crown ethers were applied to the Wurster's crowns, and the results were compared to those obtained from DFT methods. Distinct problems were found with the RHF calculated molecular geometries of the electron-rich ligand and the relative binding enthalpies of related crown ethers. The DFT methods appeared to provide results that were in better agreement with experimental results. Finally, while this paper addresses fundamental properties associated with a specific member of the Wurster's crowns, it also serves as a benchmark for future studies on other members of this versatile new class of macrocycles.

Acknowledgment. Acknowledgment is made to the donors of the Petroleum Research Fund, administered by the American Chemical Society (grant no. 33590-B5 to A.L.S.), for partial support of this research, and to the Robert A. Welch Foundation (grant no. AT-1527 to J.W.S.). We also thank the North Carolina Supercomputer Center and the ECU Center for Applied Computational Studies (CACS) for their continued support of this research.

Supporting Information Available: Tables of the Cartesian coordinates of the optimized molecular geometries for complexes 1–19 (except 3). This material is available free of charge via the Internet at <http://pubs.acs.org>.

References and Notes

- (1) (a) Sibert, J. W. U.S. Patent 6,262,258, 2001. (b) Sibert, John W. U.S. Patent 6,441,164, 2002. (c) Sibert, J. W.; Forshee, P. B. *Inorg. Chem.* **2002**, *41*, 5928–5930. (d) Sibert, J. W.; Seyer, D. J.; Hundt, G. R. *J. Supramol. Chem.* **2002**, *2*, 335–342. (e) Sibert, J. W.; Forshee, P. B.; Hundt, G. R.; Sargent, A. L.; Bott, S.; Lynch, V. *Inorg. Chem.* Submitted.
- (2) (a) Zhang, X.-X.; Buchwald, S. L. *J. Org. Chem.* **2000**, *65*, 8027–8031.
- (3) (a) Pearson, A. J.; Hwang, J. *Tetrahedron Lett.* **2001**, *41*, 3533–3536. (b) Pearson, A. J.; Hwang, J.; Ignatov, M. E. *Tetrahedron Lett.* **2001**, *41*, 3537–3540. (c) Pearson, A. J.; Hwang, J. *Tetrahedron Lett.* **2001**, *41*, 3541–3543.
- (4) (a) Crochet, P.; Malval, J.-P.; Lapouyade, R. *J. Chem. Soc., Chem. Commun.* **2000**, 289–290. (b) Malval, J.-P.; Chaimbault, C.; Fischer, B.; Morand, J.-P.; Lapouyade, R. *Res. Chem. Intermed.* **2001**, *27* (1, 2), 21–34.
- (5) (a) Wurster, C. *Ber. Dtsch. Chem. Ges.* **1879**, *12*, 522. (b) Wurster, C. *Ber. Dtsch. Chem. Ges.* **1879**, *12*, 2071. (c) Wurster, C.; Schobig, E. *Ber. Dtsch. Chem. Ges.* **1879**, *12*, 1807.

- (6) (a) Prasanna de Silva, A.; Gunaratne, H. Q. N.; Gunnaugsson, T.; Huxley, A. J. M.; McCoy, C. P.; Rademacher, J. T.; Rice, T. E. *Chem. Rev.* **1997**, *97*, 1515–1566. (b) Hayashita, T.; Takagi, M. In *Comprehensive Supramolecular Chemistry*; Gokel, G. W., Atwood, J. L., Davies, J. E., MacNicol, D. D., Vögtle, F., Eds.; Pergamon: Oxford, 1996; Vol. 1, pp 635–669.
- (7) Glendening, E. D.; Feller, D.; Thompson, M. A. *J. Am. Chem. Soc.* **1994**, *116*, 10657–10669.
- (8) (a) Bagatur'yants, A. A.; Freidzon, A. Y.; Alfimov, M. V.; Baerends, E. J.; Howard, J. A. K.; Kuz'mina, L. G. *THEOCHEM* **2002**, *588*, 55–69. (b) Stoyanov, E. S.; Reed, C. A. *J. Phys. Chem. A* **2004**, *108*, 907–913.
- (9) (a) Golebiowski, J.; Lamare, V.; Ruiz-López, M. F. *J. Comput. Chem.* **2002**, *23*, 724–731. (b) Gonzalez-Lorenzo, M.; Platas-Inglesias, C.; Aveciolla, F.; Faulkner, S.; Pope, S. J.; de Blas, A.; Rodriguez-Blas, T. *Inorg. Chem.* **2005**, *44*, 4254–4262. (c) Liddle, S. T.; Clegg, W.; Morrison, C. A. *J. Chem. Soc., Dalton Trans.* **2004**, *16*, 2514–2525. (d) Soto-Castro, D.; Guadarrama, P. *J. Comput. Chem.* **2004**, *25*, 1215–1226.
- (10) (a) Haeberlein, M.; Murray, J. S.; Brinck, T.; Politzer, P. *Can. J. Chem.* **1992**, *70*, 2209–2214. (b) Sponer, J.; Hobza, P. *Int. J. Quantum Chem.* **1996**, *57*, 959–970.
- (11) (a) Barfield, M.; Fagerness, P. *J. Am. Chem. Soc.* **1997**, *119*, 8699–8711. (b) Tzeng, W. B.; Narayanan, K. *J. Mol. Struct.* **1998**, *446*, 93–102.
- (12) Peng, C.; Ayala, P. Y.; Schlegel, H. B.; Frisch, M. J. *J. Comput. Chem.* **1996**, *17*, 49–56.
- (13) Hay, P. J.; Wadt, W. R. *J. Chem. Phys.* **1985**, *82*, 299–310.
- (14) Becke, A. D. *J. Chem. Phys.* **1993**, *98*, 5648–5652.
- (15) Lee, C.; Yang, W.; Parr, R. G. *Phys. Rev. B* **1988**, *37*, 785–789.
- (16) (a) Brouwer, A. M.; Wilbrandt, R. *J. Phys. Chem.* **1996**, *100*, 9678–9688. (b) Brouwer, A. M. *J. Phys. Chem. A* **1997**, *101*, 3626–3633.
- (17) Ikemoto, I.; Katagiri, G.; Nishimura, S.; Yakushi, K.; Kuroda, H. *Acta Crystallogr., Sect. B* **1979**, *35*, 2264–2265.
- (18) Frisch, M. J.; Trucks, G. W.; Schlegel, H. B.; Gill, P. M. W.; Johnson, B. G.; Robb, M. A.; Cheeseman, J. R.; Keith, T. A.; Petersson, G. A.; Montgomery, J. A.; Raghavachari, K.; Al-Laham, M. A.; Zakrzewski, V. G.; Ortiz, J. V.; Foresman, J. B.; Cioslowski, J.; Stefanov, B. B.; Nanayakkara, A.; Challacombe, M.; Peng, C. Y.; Ayala, P. Y.; Chen, W.; Wong, M. W.; Andres, J. L.; Replogle, E. S.; Gomperts, R.; Martin, R. L.; Fox, D. J.; Binkley, J. S.; Defrees, D. J.; Baker, J.; Stewart, J. J. P.; Head-Gordon, M.; Gonzalez, C.; Pople, J. A. *Gaussian 94*, revision D1; Gaussian, Inc.: Pittsburgh, PA, 1995.
- (19) Frisch, M. J.; Trucks, G. W.; Schlegel, H. B.; Scuseria, G. E.; Robb, M. A.; Cheeseman, J. R.; Zakrzewski, V. G.; Montgomery, J. A., Jr.; Stratmann, R. E.; Burant, J. C.; Dapprich, S.; Millam, J. M.; Daniels, A. D.; Kudin, K. N.; Strain, M. C.; Farkas, O.; Tomasi, J.; Barone, V.; Cossi, M.; Cammi, R.; Mennucci, B.; Pomelli, C.; Adamo, C.; Clifford, S.; Ochterski, J.; Petersson, G. A.; Ayala, P. Y.; Cui, Q.; Morokuma, K.; Malick, D. K.; Rabuck, A. D.; Raghavachari, K.; Foresman, J. B.; Chioslowski, J.; Ortiz, J. V.; Baboul, A. G.; Stefanov, B. B.; Liu, G.; Liashenko, A.; Piskorz, P.; Komaromi, I.; Gomperts, R.; Martin, R. L.; Fox, D. J.; Keith, T.; Al-Laham, M. A.; Peng, C. Y.; Nanayakkara, A.; Challacombe, M.; Gill, P. M. W.; Johnson, B.; Chen, W.; Wong, M. W.; Andres, J. L.; Gonzalez, C.; Head-Gordon, M.; Replogle, E. S.; Pople, J. A. *Gaussian 98*, revision A.9; Gaussian Inc.: Pittsburgh, PA, 1998.
- (20) Boys, S. F.; Bernardi, F. *Mol. Phys.* **1970**, *19*, 553–566.
- (21) Del Bene, J. E.; Mettee, H. D.; Frisch, M. J.; Kuke, B. T.; Pople, J. A. *J. Phys. Chem.* **1983**, *87*, 3279–3282.
- (22) Reed, A. E.; Curtiss, L. A.; Weinhold, F. *Chem. Rev.* **1988**, *88*, 899–926.
- (23) Interactive MOPLOT incorporates the programs MOPLOT (Lichtenberger, D.), PLOTDEN (Bader, R. F. W.; Kenworthy, D. J.; Beddal, P. M.; Runtz, G. R.; Anderson, S. G.), SCHUSS (Bader, R. F. W.; Runtz, G. R.; Anderson, S. G.; Biegler-Koenig, F. W.), and EXTREM (Bader, R. F. W.; Biegler-Koenig, F. W.) Sherwood, P.; MacDougall, P. J. 1989. Contact Dr. Preston J. MacDougall, Department of Chemistry, Middle Tennessee State University, Murfreesboro, TN 37132 for details.
- (24) A recent report (Al-Jallel, N. A.; Al-Kahtani, A. A.; El-Azhary, A. A. *J. Phys. Chem. A* **2005**, *109*, 3694–3703) suggests that an S_6 symmetry isomer is lower energy than the C_i conformation in the gas-phase based on MP2/6-31+G* calculations. However, our own calculations at the higher G3MP2 level of theory demonstrate that the C_i conformation is lower in energy (the G3MP2 energy, enthalpy, and free energy, in hartrees, for the C_i conformation are –921.561 986, –921.561 042, and –921.632 514, respectively, while those for the S_6 conformation are –921.561 614, –921.560 670, and –921.630 660). Cartesian coordinates for both conformations are listed in the Supporting Information.
- (25) For example, see Rurack, K.; Bricks, J. L.; Reck, G.; Radeaglia, R.; Resch-Genger, U. *J. Phys. Chem. A* **2000**, *101*, 3087–3109.
- (26) An interesting example of an apparent “tangential” Na^+ complex with an aniline-containing crown ether has been reported. Lu, X.; Zhong, R.; Liu, S.; Liu, Y. *Polyhedron* **1997**, *16* (21), 3865–3872.
- (27) Aoki, S.; Kagata, D.; Shiro, M.; Takeda, K.; Kimura, E. *J. Am. Chem. Soc.* **2004**, *126*, 13377–13390 and references therein.
- (28) Frensdorf, H. K. *J. Am. Chem. Soc.* **1971**, *93*, 600.
- (29) Dehareng, D.; Dive, G.; Moradpour, A. *Int. J. Quantum Chem.* **2000**, *76*, 552–573.
- (30) Abe, J.; Miyazaki, T.; Takahashi, H. *J. Chem. Phys.* **1989**, *90*, 2317–2319.
- (31) Na^+ and Mg^{2+} complexes of the electroactive *N*-phenylaza-15-crown-5 also show a pronounced anodic shift. Mortimer, R. J.; Weightman, J. S. *J. Electroanal. Chem.* **1996**, *418*, 1–7.
- (32) Le Derf, F.; Mazari, M.; Mercier, N.; Levillain, E.; Richomme, P.; Becher, J.; Garín, J.; Orduna, J.; Gorgues, A.; Sallé, M. *Inorg. Chem.* **1999**, *38*, 6096–6100.
- (33) It should be emphasized here that, although the ΔH values calculated for the K^+ , Rb^+ , and Cs^+ complexes of $w18c6^+$ are small and positive, the gas-phase approximation inherent in the calculation carries with it an error of potentially several kcal/mol regarding the absolute value of the binding enthalpy and therefore does not preclude a weakly bound complex.
- (34) More, M. B.; Ray, D.; Armentrout, P. B. *J. Am. Chem. Soc.* **1999**, *121*, 417–423.
- (35) Kaifer, A. E.; Gustowski, D. A.; Echegoyen, L.; Gatto, V. J.; Schultz, R. A.; Cleary, T. P.; Morgan, C. R.; Rios, A. M.; Gokel, G. W. *J. Am. Chem. Soc.* **1985**, *107*, 1958.
- (36) Glendening, E. D.; Feller, D. *J. Phys. Chem.* **1995**, *99*, 3060–3067.